Korean J. Chem. Eng., 34(5), 1475-1482 (2017)
DOI: 10.1007/s11814-017-0038-9

pISSN: 0256-1115
eISSN: 1975-7220

The effect of cyano groups on the solubility of carbon dioxide in ionic liquids containing cyano groups in anion

Hang-Kyu Cho, Ji Eun Kim, and Jong Sung Lim†

Department of Chemical and Biomolecular Engineering, Sogang University, C. P. O. Box 1142, Seoul 04107, Korea
(*Received 30 December 2016 • accepted 9 February 2017*)

Abstract−The solubility of carbon dioxide (CO_2) was investigated using three ionic liquids containing different numbers of cyano groups in the anion, 1-hexyl-3-methylimidazolium tricyanomethanide ($[c_6mim][C(CN)_3]$), 1-hexyl-3-methylimidazolium dicyanamide ($[c_6mim][N(CN)_2]$), and 1-hexyl-3-methylimidazolium thiocyanate ($[c_6mim][SCN]$). The CO_2 solubilities were determined by measuring the bubble point pressures of the CO_2+ionic liquid mixtures at temperatures ranging from 303.15 to 373.15 K and pressure up to 105 MPa. The experimental results showed that the solubilities of CO_2 in ionic liquids increased with pressure, decreased with temperature, and increased with the length of the alkyl chains in the cation. Furthermore, a higher CO_2 solubility was achieved in the ionic liquid with more cyano groups in the anion. The experimental data were correlated with the Peng-Robinson equation of state (PR-EoS), using the conventional van der Waals one fluid mixing rule and the modified Lydersen-Joback-Reid method. The average absolute deviation values of pressure (AAD-P) were 0.0658 for CO_2+$[c_6mim][SCN]$, 0.0633 for CO_2+$[c_6mim][N(CN)_2]$, and 0.0761 for CO_2+$[c_6mim][C(CN)_3]$ system.

Keywords: Ionic Liquids, $[c_6mim][C(CN)_3]$, $[c_6mim][N(CN)_2]$, $[c_6mim][SCN]$, CO_2 Solubility, CO_2 Capture, Cyano Group

INTRODUCTION

Carbon dioxide is said to contribute more than 60% to global warming [1], resulting in climate change, which is of global concern. Carbon capture and storage (CCS) is considered one of the most promising solutions to decrease the amount of CO_2 in the atmosphere [2-4]. Aqueous amine-based solvents, such as monoethanolamine (MEA), diethanolamine (DEA), and n-methyldiethanolamine (MDEA), are currently used as CO_2-absorbing solvents in many industrial CO_2-capturing processes [5]. However, these amine-based solvents have several disadvantages. Owing to their high (70-80 wt%) aqueous content, considerable energy is required in the heating process to regenerate the amine absorbent after the CO_2 is absorbed. Furthermore, some amine absorbents are pyrolyzed and show increased corrosiveness at high temperatures. These drawbacks not only increase the cost of the process but also pose harm to the environment [6]. To overcome these disadvantages, alternative CO_2 capture solvents have been studied as third-generation CO_2 capture solvents. Ionic liquids have received much attention among these novel classes of solvents [7-9]. In contrast to amine-based solvents, some ionic liquids used for CO_2 capture are anhydrous; thus, these ionic liquids need less energy to be recycled than do aqueous amine-based solvents [10]. In addition, IEA GHG [11] has shown that ionic liquids provide remarkable solubility of CO_2. Some ionic liquids exhibit 40-times greater CO_2 solubility than MEA [11], which is the most popular and conventional among commonly available solvents [12,13]. Moreover, some ionic liquids could be directly applied in the same type of equipment which is designed for amine-based solvents [10]. Therefore, many researchers have studied ionic liquids as a new CO_2 absorbent.

To design ionic liquids showing appreciable solubility of CO_2, many studies are under way for measuring the solubility of CO_2 in many kinds of ionic liquids such as conventional ILs, task-specific ILs, and reversible ILs [13]. Furthermore, recent studies have focused on supported ionic liquid membranes (SILMs) [14-20] and a mixture of ionic liquids and amines to improve the performance of ionic liquids [21-25]. Cadena et al. [26] studied the solubilities of CO_2 in imidazolium-based ionic liquids and found that anions play an important role in the interaction with CO_2. In addition, other research groups demonstrated that anions containing fluorine improve the solubility of CO_2 [27,28]. Therefore, it is necessary to continue investigating CO_2 solubilities in many different ionic liquids. To date, we have studied the solubilities of CO_2 in various ionic liquids, and recently reported the solubilities of CO_2 in ionic liquids containing cyano groups in their anions: $[c_2mim][SCN]$, $[c_2mim][N(CN)_2]$, $[c_2mim][C(CN)_3]$, $[c_4mim][SCN]$, $[c_4mim][N(CN)_2]$, and $[c_4mim][C(CN)_3]$ [29,30].

In this study, we measured the solubilities of CO_2 in ionic liquids with anions containing cyano groups, 1-hexyl-3-methylimidazolium thiocyanate ($[c_6mim][SCN]$), 1-hexyl-3-methylimidazolium dicyanamide ($[c_6mim][N(CN)_2]$), and 1-hexyl-3-methylimidazolium tricyanomethanide ($[c_6mim][C(CN)_3]$), to clarify the phase behavior of CO_2 in three different ionic liquids. The solubility of CO_2 was determined by measuring the bubble-point pressure (or cloud-point pressure) at a fixed temperature. The range of temperatures for the experimental measurements was 303.15-373.15 K at 10 K intervals.

†To whom correspondence should be addressed.
E-mail: limjs@sogang.ac.kr
‡This article is dedicated to Prof. Ki-Pung Yoo on the occasion of his retirement from Sogang University.

Table 1. Chemical structure and purity data of ionic liquids and CO_2

Structure	Source	Assay (Mass%)	Halides content (%)	Initial water content (PPM)	Water removal method	Final water content (PPM)	Water analysis method
CO_2	Dong-A Gas Co.	99.999	-	-	-	-	-
$[c_6mim][SCN]$ 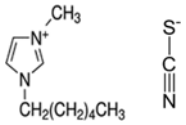	Future-Chem	>98	2.00	730	Vacuum evaporation	19	Karl Fischer titration
$[c_6mim][N(CN)_2]$ 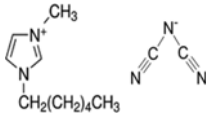	Future-Chem	>98	2.00	20530	Vacuum evaporation	29	Karl Fischer titration
$[c_6mim][C(CN)_3]$ 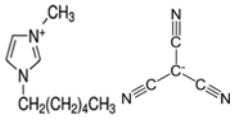	Future-Chem	>98	0.50	348	Vacuum evaporation	18	Karl Fischer titration

The experimental data were correlated with the Peng-Robbins equation of state (PR-EoS), using the conventional van der Waals one-fluid mixing rules. We used the modified Lydersen-Joback-Reid method to estimate the critical properties and acentric factor of the ionic liquids. Thereon, we investigated the effects of the number of cyano groups in the anion and the length of the alkyl chains in the cation on the solubility of CO_2.

EXPERIMENTAL

1. Chemicals

Ionic liquids $[c_6mim][SCN]$, $[c_6mim][N(CN)_2]$ and $[c_6mim][C(CN)_3]$ were purchased from FutureChem (Korea). The chemical structure and the purity data of ionic liquids are shown in Table 1. The purity data by the HPLC analysis were provided by the supplier. To reduce the water content and to eliminate the other gases in ionic liquids, they were evacuated by vacuum pump for at least 24 hour before measurement. Coulometric Karl Fischer titration (Metrohm model 684) was performed on a sample of the evacuated ionic liquids to analyze the final water content after evacuation. All the resulting water content of ionic liquids was under 29 ppm. High-grade of CO_2 (99.999 mass%) was used for measurement of CO_2 solubility. The ionic liquids and CO_2 gas were used without further purification.

2. Experimental Apparatus and Procedure

The solubility of CO_2 in ionic liquids was measured with a high-pressure apparatus equipped with a variable-volume view cell. A schematic diagram of the experimental apparatus is shown in Fig. 1. A detailed explanation of the experimental apparatus and procedure can be obtained from our previous publication [29-33].

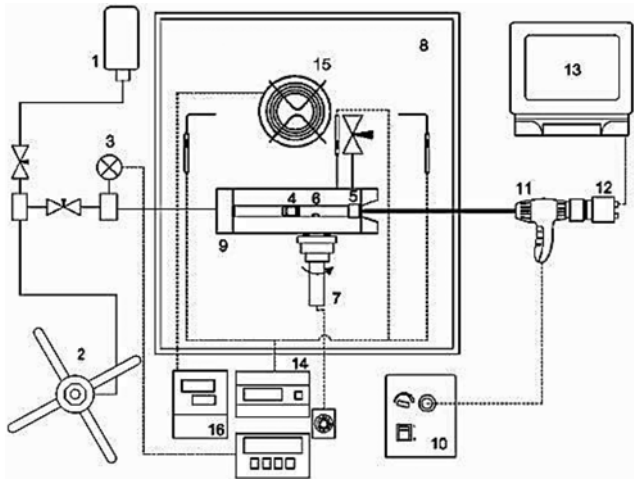

Fig. 1. A schematic diagram of the experimental apparatus.

1. Water for pressing	9. Variable-volume view cell
2. Pressure generator	10. Light source
3. Pressure gauge	11. Borescope
4. Piston	12. CCD camera
5. Sapphire window	13. Monitor
6. Magnetic bar	14. Temperature gauge
7. Stirrer	15. Heater
8. Air bath	16. Heating controller

CORRELATION

The experimental (CO_2+ionic liquid) data were correlated with the Peng-Robinson equation of state (PR-EoS) [34]. The mixture parameters in ionic liquid phase were calculated with the conventional van der Waals one-fluid mixing rules. A detailed explanation of the PR-EoS and the conventional van der Waals one-fluid mixing rules was reported in our previous works [31-33]. To calculate the parameters of the PR-EoS, the normal boiling temperature (T_b), critical temperature (T_c), critical pressure (P_c) and acentric factor (ω) of the ionic liquids and CO_2 are needed. Those properties of CO_2 can be easily obtained from the literature [35]; however, those of ionic liquids are not available. Therefore, the critical properties of the ionic liquids must be estimated. We used the modified Lydersen-Joback-Reid method [36], which is a group contribution method, to estimate the critical temperature (T_c) and critical pressure (P_c)

for the ionic liquids. The groups considered for the modified Lydersen-Joback-Reid method are presented in literature [36]. The acentric factor was calculated from the critical properties and the normal boiling temperature (T_b for P_b=0.1 MPa). All the calculated critical properties, the normal boiling temperature and the acentric factors of the ionic liquids are listed in Table 2 along with those of CO_2.

RESULTS AND DISCUSSION

The solubility of carbon dioxide in ionic liquids with anions containing three different numbers of cyano groups, [$c_6$mim][SCN], [$c_6$mim][$N(CN)_2$] and [$c_6$mim][$C(CN)_3$] was measured at five equally spaced temperatures between 303.15 and 373.15 K. To dissolve the CO_2 gas into the ionic liquids, the solution (ionic liquid+

Table 2. The critical properties and acentric factor of CO_2 from literature [35] and ionic liquids calculated from the modified Lydersen-Joback-Reid method [36]

	M/(g·mol^{-1})	T_b/K	T_c/K	P_c/MPa	ω
CO_2	44	-	304.21	7.3847	0.2239
[$c_6$mim][SCN]	225.35	808.84	1082.13	1.7164	0.5647
[$c_6$mim][$N(CN)_2$]	254.08	828.72	1073.82	2.2866	0.9723
[$c_6$mim][$C(CN)_3$]	257.33	960.82	1222.41	1.8530	0.9983

Table 3. Solubility data for the [$c_6$mim][SCN]+CO_2 system[a]

x_{CO_2}	T/K	P/MPa	Phase state of CO_2	x_{CO_2}	T/K	P/MPa	Phase state of CO_2
0.148	303.15	0.89	b[b]	0.518	303.15	21.25	c[c]
	313.15	1.13	b		313.15	24.76	c
	323.15	1.42	b		323.15	27.95	c
	333.15	1.68	b		333.15	30.69	c
	343.15	2.15	b		343.15	33.25	c
	353.15	2.38	b		353.15	35.82	c
	363.15	2.64	b		363.15	37.66	c
	373.15	2.98	b		373.15	39.63	c
0.261	303.15	2.07	b	0.562	303.15	42.85	c
	313.15	2.37	b		313.15	45.85	c
	323.15	2.81	b		323.15	48.57	c
	333.15	3.26	b		333.15	51.52	c
	343.15	3.88	b		343.15	53.84	c
	353.15	4.57	b		353.15	56.02	c
	363.15	5.28	b		363.15	58.08	c
	373.15	5.91	b		373.15	60.02	c
0.360	303.15	3.33	b	0.593	303.15	60.74	c
	313.15	3.82	b		313.15	64.01	c
	323.15	4.64	b		323.15	66.98	c
	333.15	5.58	b		333.15	69.21	c
	343.15	6.86	b		343.15	71.63	c
	353.15	8.18	b		353.15	73.81	c
	363.15	9.64	b		363.15	75.65	c
	373.15	11.11	b		373.15	77.41	c
0.457	303.15	5.70	b	0.611	303.15	77.77	c
	313.15	7.49	b		313.15	80.26	c
	323.15	10.07	b		323.15	82.32	c
	333.15	13.20	b		333.15	84.49	c
	343.15	15.37	b		343.15	86.11	c
	353.15	17.99	b		353.15	87.96	c
	363.15	20.43	b		363.15	89.61	c
	373.15	22.69	b		373.15	91.23	c

[a]Standard uncertainties u are u(T)=0.1 K, u(P)=0.05 MPa and u(x)=0.007 mole fractions

[b]Bubble point

[c]Cloud point

Table 4. Solubility data for the $[c_6mim][N(CN)_2]+CO_2$ system[a]

x_{CO_2}	T/K	P/MPa	Phase state of CO_2	x_{CO_2}	T/K	P/MPa	Phase state of CO_2
0.209	303.15	0.68	b[b]	0.665	303.15	19.07	c[c]
	313.15	0.88	b		313.15	24.57	c
	323.15	1.13	b		323.15	29.35	c
	333.15	1.47	b		333.15	34.33	c
	343.15	1.77	b		343.15	39.00	c
	353.15	2.16	b		353.15	42.83	c
	363.15	2.47	b		363.15	46.16	c
	373.15	2.78	b		373.15	49.44	c
0.291	303.15	1.68	b	0.701	303.15	35.35	c
	313.15	2.00	b		313.15	41.21	c
	323.15	2.35	b		323.15	46.32	c
	333.15	2.87	b		333.15	50.87	c
	343.15	3.38	b		343.15	55.05	c
	353.15	3.85	b		353.15	58.42	c
	363.15	4.38	b		363.15	61.05	c
	373.15	5.02	b		373.15	64.59	c
0.418	303.15	2.97	b	0.714	303.15	58.79	c
	313.15	3.61	b		313.15	64.79	c
	323.15	4.39	b		323.15	70.24	c
	333.15	5.37	b		333.15	75.14	c
	343.15	6.33	b		343.15	79.74	c
	353.15	7.29	b		353.15	83.74	c
	363.15	8.44	b		363.15	87.20	c
	373.15	9.63	b		373.15	90.59	c
0.549	303.15	4.98	b	0.723	303.15	70.02	c
	313.15	6.00	b		313.15	76.08	c
	323.15	7.89	b		323.15	81.45	c
	333.15	9.96	b		333.15	86.44	c
	343.15	11.92	b		343.15	90.64	c
	353.15	14.32	b		353.15	95.13	c
	363.15	16.70	b		363.15	98.47	c
	373.15	19.26	b		373.15	101.76	c
0.611	303.15	7.40	c[c]				
	313.15	11.46	c				
	323.15	15.48	c				
	333.15	19.37	c				
	343.15	23.13	c				
	353.15	26.14	c				
	363.15	29.14	c				
	373.15	32.16	c				

[a]Standard uncertainties u are u(T)=0.1 K, u(P)=0.05 MPa and u(x)=0.007 mole fractions
[b]Bubble point
[c]Cloud point

CO_2) in the cell was consistently pressurized until it became a homogeneous single phase. After then, the solution was slowly depressurized until the first gas bubble separated from the liquid solution was observed, and we considered this point as the bubble point. For a solution of a relatively high CO_2 mole fraction, cloud point behavior was observed rather than bubble point behavior. At a cloud point, the solution becomes cloudy due to the phase transition from a single phase to liquid-liquid two phases. We defined the cloud point as the pressure at which we could no longer visually observe the motion of stirring bar in the cell. The experimental results for the CO_2+$[c_6mim][SCN]$, +$[c_6mim][N(CN)_2]$, and +$[c_6mim][C(CN)_3]$ are shown in Tables 3-5, respectively. These tables represent the measured bubble-point or cloud-point pressures at fixed CO_2 mole fractions and temperatures. When the CO_2 mole fraction was equal to or less than 0.457 for the CO_2+$[c_6mim][SCN]$, 0.549 for the CO_2+$[c_6mim][N(CN)_2]$ and 0.629 for the CO_2+

Table 5. Solubility data for the $[c_6mim][C(CN)_3]+CO_2$ system[a]

x_{CO_2}	T/K	P/MPa	Phase state of CO_2	x_{CO_2}	T/K	P/MPa	Phase state of CO_2
0.208	303.15	0.59	b[b]	0.629	303.15	5.46	b
	313.15	0.81	b		313.15	6.91	b
	323.15	1.01	b		323.15	9.68	b
	333.15	1.24	b		333.15	12.53	b
	343.15	1.49	b		343.15	15.58	b
	353.15	1.69	b		353.15	18.56	b
	363.15	1.95	b		363.15	21.73	b
	373.15	2.17	b		373.15	24.53	b
0.311	303.15	1.27	b	0.679	303.15	10.82	c[c]
	313.15	1.69	b		313.15	16.37	c
	323.15	1.96	b		323.15	20.68	c
	333.15	2.25	b		333.15	25.22	c
	343.15	2.64	b		343.15	29.44	c
	353.15	3.01	b		353.15	32.95	c
	363.15	3.41	b		363.15	35.72	c
	373.15	3.82	b		373.15	39.37	c
0.405	303.15	2.26	b	0.718	303.15	27.84	c[c]
	313.15	2.57	b		313.15	31.98	c
	323.15	2.99	b		323.15	37.12	c
	333.15	3.35	b		333.15	42.14	c
	343.15	3.84	b		343.15	46.75	c
	353.15	4.32	b		353.15	50.22	c
	363.15	5.11	b		363.15	54.46	c
	373.15	5.85	b		373.15	57.43	c
0.494	303.15	3.26	b	0.746	303.15	46.32	c[c]
	313.15	3.93	b		313.15	51.47	c
	323.15	4.74	b		323.15	55.96	c
	333.15	5.52	b		333.15	61.09	c
	343.15	6.21	b		343.15	65.02	c
	353.15	7.46	b		353.15	68.77	c
	363.15	8.49	b		363.15	72.21	c
	373.15	9.82	b		373.15	75.65	c
0.568	303.15	4.00	b	0.776	303.15	79.00	c
	313.15	4.86	b		313.15	83.07	c
	323.15	6.06	b		323.15	88.24	c
	333.15	7.64	b		333.15	91.56	c
	343.15	9.20	b		343.15	95.54	c
	353.15	10.77	b		353.15	98.91	c
	363.15	12.80	b		363.15	102.08	c
	373.15	15.44	b		373.15	105.01	c

[a]Standard uncertainties u are u(T)=0.1 K, u(P)=0.05 MPa and u(x)=0.007 mole fractions
[b]Bubble point
[c]Cloud point

$[c_6mim][C(CN)_3]$ system, bubble-point behavior was observed when the phase separations occurred. On the other hand, when the CO_2 mole fraction was equal to or greater than 0.518 for the CO_2+$[c_6mim][SCN]$, 0.665 for the CO_2+$[c_6mim][N(CN)_2]$ and 0.679 for the CO_2+$[c_6mim][C(CN)_3]$ system, cloud-point behavior was observed. Fig. 2 illustrates the relationship between the equilibrium pressure and temperature at various CO_2 mole fractions. The bubble-point or cloud-point pressure increased linearly with the system temperature at a fixed mole fraction of CO_2. This means that the solubility of CO_2 in the ionic liquid increased with the system temperature. The slope of the bubble-point or cloud-point pressure versus temperature, $(\partial P/\partial T)_{x1}$, increased as the mole fraction of CO_2 increased. This also means that the solubility of CO_2 in the ionic liquid decreased with increasing the CO_2 mole fraction.

When the mole fraction of CO_2 increased isothermally, the equilibrium pressure increased significantly. This can be seen more eas-

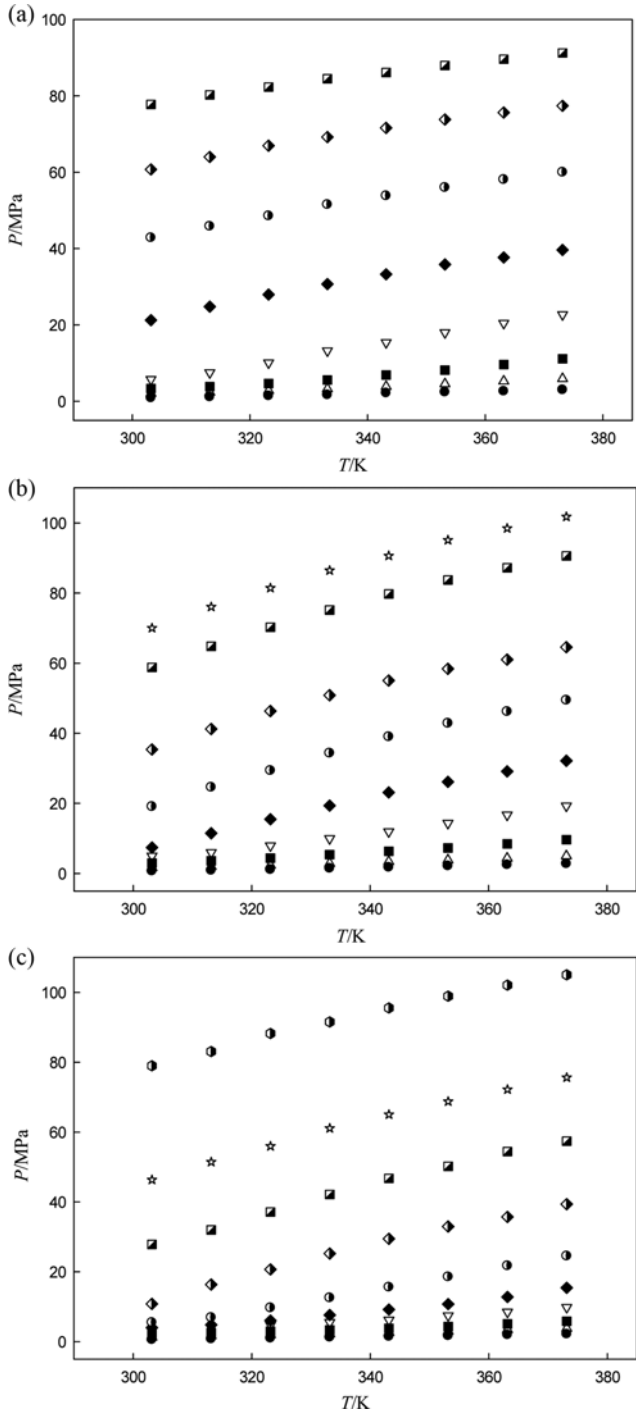

Fig. 2. P-T diagram of CO_2 solubilities of the (ionic liquid+CO_2) system: (a) [$c_6$mim][SCN]+CO_2. The symbols are CO_2 mole fraction; (●) 0.148, (△) 0.261, (■) 0.360, (▽) 0.457, (◆) 0.518, (◑) 0.562, (◈) 0.593, (◪) 0.611: (b) [$c_6$mim][$N(CN)_2$]+CO_2; (●) 0.209, (△) 0.291, (■) 0.418, (▽) 0.549, (◆) 0.611, (◑) 0.665, (◈) 0.701, (◪) 0.714, (☆) 0.723: (c) [$c_6$mim][$C(CN)_3$]+CO_2; (●) 0.208, (△) 0.311, (■) 0.405, (▽) 0.494, (◆) 0.568, (◑) 0.629, (◈) 0.679, (◪) 0.718, (☆) 0.746, (◈) 0.776.

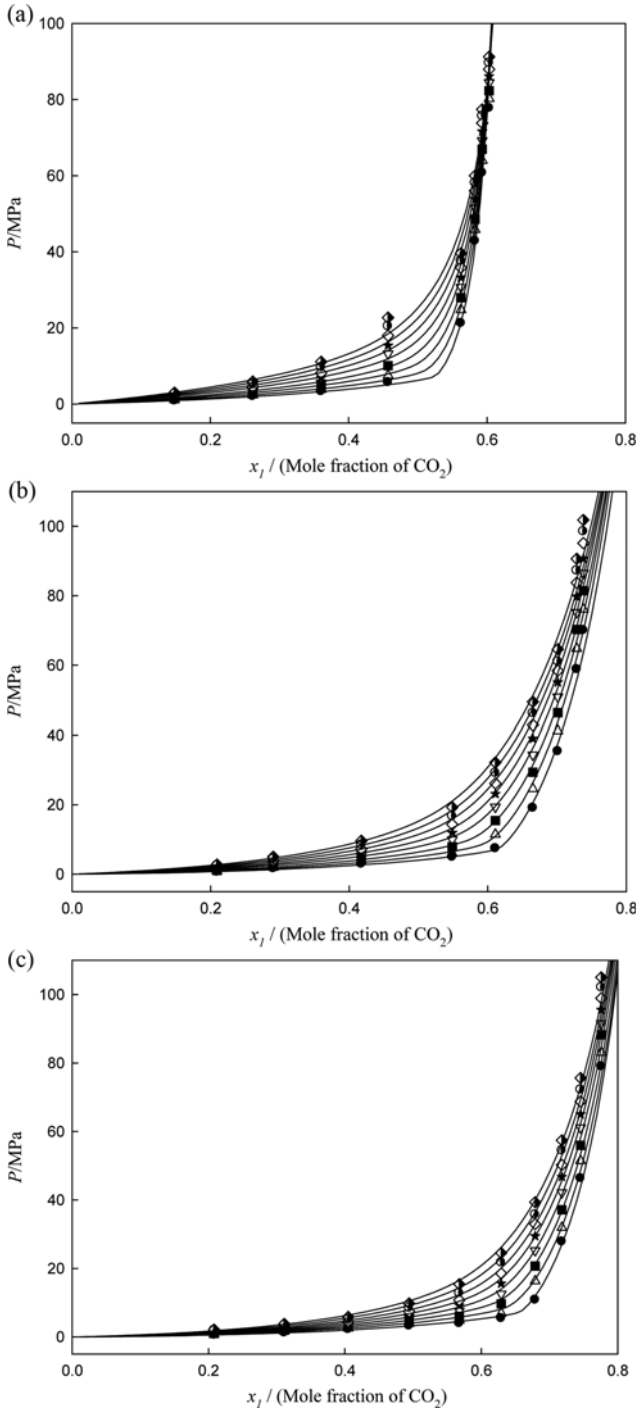

Fig. 3. P-x_1 diagram of CO_2 solubilities of the (ionic liquid+CO_2) system: (a) [$c_6$mim][SCN]; (b) [$c_6$mim][$N(CN)_2$]; (c) [$c_6$mim][$C(CN)_3$]+CO_2. The symbols are temperature; (●) 303.15 K, (△) 313.15 K, (■) 323.15 K, (▽) 333.15 K, (★) 343.15 K, (◇) 353.15 K, (◑) 363.15 K, (◆) 373.15 K; (-) calculated by the PR-EoS.

ily from a P-x_1 diagram in which the bubble-point or cloud-point pressure is plotted against CO_2 mole fraction at a fixed temperature. Fig. 3 shows the P-x_1 diagrams at fixed eight temperatures from 303.15 to 373.15 K for the (a) CO_2+[$c_6$mim][SCN], (b) CO_2+[$c_6$mim][$N(CN)_2$], and (c) CO_2+[$c_6$mim][$C(CN)_3$] systems. Each figure represents the solubilities of CO_2 in each ionic liquid as a function of pressure at various temperatures. At a region of relatively low mole

Table 6. Binary interaction parameters (k_{12}, l_{12}) for the ionic liquids system

Temperature	[$c_6$mim][SCN]		[$c_6$mim][N(CN)$_2$]		[$c_6$mim][C(CN)$_3$]	
	k_{12}	l_{12}	k_{12}	l_{12}	k_{12}	l_{12}
303.15 K	0.1626	0.0293	0.0672	0.0405	0.0668	0.0380
313.15 K	0.1671	0.028	0.0694	0.0405	0.0674	0.0372
323.15 K	0.1688	0.0249	0.0708	0.0400	0.0695	0.0384
333.15 K	0.1730	0.0234	0.0711	0.0381	0.0720	0.0401
343.15 K	0.1699	0.0176	0.0730	0.0386	0.0742	0.0416
353.15 K	0.1743	0.0163	0.0742	0.0386	0.0762	0.0431
363.15 K	0.1787	0.0153	0.0758	0.0392	0.0774	0.0435
373.15 K	0.1832	0.0143	0.0777	0.0398	0.0789	0.0440

Table 7. Average absolute deviations of pressure (AAD-P %) between experimental data and calculated values for the ionic liquid+ CO_2 systems[a]

Temperature	[b]AAD-P %		
	[$c_6$mim][SCN]	[$c_6$mim][N(CN)$_2$]	[$c_6$mim][C(CN)$_3$]
303.15 K	4.57	8.59	7.43
313.15 K	5.03	7.85	7.67
323.15 K	6.66	6.16	7.42
333.15 K	7.49	5.63	7.70
343.15 K	7.77	5.49	8.51
353.15 K	6.36	5.68	8.10
363.15 K	7.07	5.75	7.69
373.15 K	7.69	5.51	6.32
Average	6.58	6.33	7.61

[a]Standard uncertainties u are u(T)=0.1 K and u(P)=0.05 MPa

[b]Average absolute deviation in percentage:

$$AAD\% = \frac{1}{N}\Sigma_{i=1}^{N}\frac{\left|p_i^{calc} - p_i^{exp}\right|}{p_i^{exp}} \times 100 \text{ (N = number of data)}$$

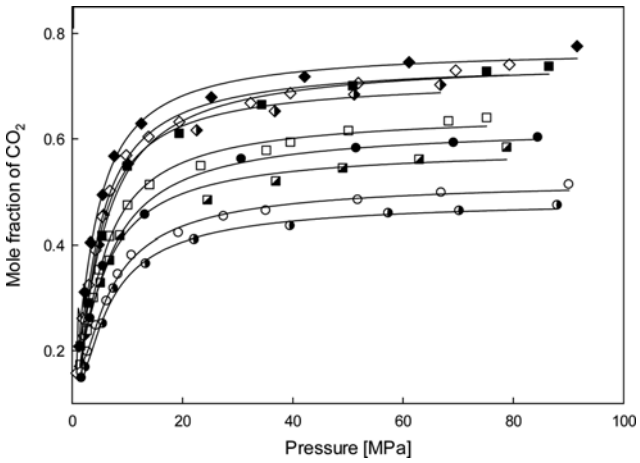

Fig. 4. Comparison of CO_2 solubilities in ionic liquids containing cyano groups in anion at 333.15 K. The symbols are ionic liquids; (◑) [$c_2$mim][SCN] [29], (◪) [$c_2$mim][N(CN)$_2$] [29], (◗) [$c_2$mim][C(CN)$_3$] [29], (○) [$c_4$mim][SCN] [30], (□) [$c_4$mim][N(CN)$_2$] [30], (◇) [$c_4$mim][C(CN)$_3$] [30], (●) [$c_6$mim][SCN], (■) [$c_6$mim][N(CN)$_2$], (◆) [$c_6$mim][C(CN)$_3$].

fraction of CO_2, the equilibrium pressures were reasonably low; however, they increased dramatically when the CO_2 mole fraction further increased. Fig. 3 also shows that the solubility of CO_2 decreases with temperature at a fixed pressure, while it increases with pressure at a fixed temperature. The comparisons between the experimental and calculated data are also illustrated in Fig. 3. The PR-EoS with the van der Waals one-fluid mixing rules was used to correlate the experimental data. The calculated binary interaction parameters for each system at eight temperatures equally spaced from 303.15 to 373.15 K are given in Table 6. Average absolute deviations of pressure (AAD-P %) between the experimental and calculated data at each temperature are shown in Table 7. The overall AAD-P values were 0.0658 for CO_2+[$c_6$mim][SCN], 0.0633 for CO_2+[$c_6$mim][N(CN)$_2$] and 0.0761 for CO_2+[$c_6$mim][C(CN)$_3$] system. These values are comparatively small and acceptable. We can conclude that the calculated results by using the PR-EoS with the van der Waals one-fluid mixing rules correspond well with the experimental data.

Fig. 4 illustrates a comparison of the CO_2 solubilities in nine different ionic liquids containing cyano groups in their anion at 333.15 K. The experimental data of [$c_2$mim]-, and [$c_4$mim]-cation based ionic liquids are referred from our previous work [29] and [30], respectively. In each system, the slopes of the CO_2 solubility curves are steep at the low pressure region. However, when the pressure further increased, they rapidly slowed although the system pressure increased continuously. This is thought to be because after a certain amount of CO_2 is dissolved, CO_2 is no longer soluble in ionic liquid because there is no more free space available to accommodate another molecule of CO_2 without disturbing the bulk structure. For the ionic liquids having the same cation, the CO_2 solubilities in ionic liquids are affected by the numbers of cyano groups in anion. For example, at a certain pressure of 60 MPa, the CO_2 solubility for CO_2+[$c_6$mim][C(CN)$_3$] system, CO_2+[$c_6$mim][N(CN)$_2$] system, and CO_2+[$c_6$mim][SCN] system was about 0.75, 0.70, and 0.6, respectively. That is, CO_2+[$c_6$mim][C(CN)$_3$] system has the highest, and CO_2+[$c_6$mim][N(CN)$_2$] has the middle, and CO_2+[$c_6$mim][SCN] has the lowest solubility of CO_2 at a fixed pressure. This means that the solubility of CO_2 in the ionic liquids having the same cation increases with the numbers of cyano groups in their anion. As can be seen in Fig. 4, this experimental result is applicable to the other ionic liquids having the same cation of [$c_2$mim] [29] and [$c_4$mim] [30]. Fig. 4 also illustrates a comparison

of CO_2 solubilities in ionic liquids having the same anion and containing different alkyl chains in cation at 333.15 K. For the ionic liquids having the same anion, the [$c_6$mim]-cation based ionic liquid has the highest solubility, while [$c_2$mim]-cation based ionic liquid has the lowest one. In other words, the solubility of CO_2 increases with increasing the length of alkyl chain in cation. Consequently, the numbers of cyano groups in anion and the length of alkyl chain in cation enhance the solubility of CO_2. As a result of the complex effects of the numbers of cyano groups in anion and the length of alkyl chain in cation, the order of magnitude of the solubility of CO_2 turned out to be [$c_6$mim][$C(CN)_3$]>[$c_4$mim][$C(CN)_3$] [30]≈[$c_6$mim][$N(CN)_2$]>[$c_2$mim][$C(CN)_3$] [29]>[$c_4$mim][$N(CN)_2$] [30]>[$c_6$mim][SCN]>[$c_2$mim][$N(CN)_2$] [29]>[$c_4$mim][SCN]>[$c_2$mim][SCN] [29].

CONCLUSION

The solubility of CO_2 in ionic liquid was measured to determine the effect of cyano groups in anion. The experimental data was correlated by the PR-EoS with the van der Waals one-fluid mixing rules. Normal boiling temperature, acentric factor and critical properties of ionic liquids were estimated by the modified Lydersen-Joback-Reid method. The experimental equilibrium pressure was comparatively well commensurate with the calculated results using the PR-EoS. The solubility of CO_2 increased with decreasing temperature and increasing pressure. Also, the solubilities of CO_2 in ionic liquids were affected by the numbers of cyano groups in their anion and the length of alkyl chain in cation. In summary, ionic liquid which contains the more numbers of cyano groups in anion and the longer alky chain in cation shows the higher solubility of CO_2.

REFERENCES

1. T. H. Oh, *Renew. Sustainable Energy Rev.*, **14**, 2697 (2010).
2. H. J. Herzog, *Energy Econ.*, **33**, 597 (2011).
3. F. M. Orr, *Energy Environ. Sci.*, **2**, 449 (2009).
4. X. Zhang, X. Zhang, H. Dong, Z. Zhao, S. Zhang and Y. Huang, *Energy Environ. Sci.*, **5**, 6668 (2012).
5. Z. Xue, Z. Zhang, J. Han, Y. Chen and T. Mu, *Int. J. Greenh, Gas Control.*, **5**, 628 (2011).
6. H. Lepaumier, D. Picq and P. L. Carrette, *Ind. Eng. Chem. Res.*, **48**, 9061 (2009).
7. M. Freemantle, An Introduction to Ionic Liquids, 1st Ed., Royal Society of Chemistry (2010).
8. K. E. *Interface Electrochem. Soc.*, **16**, 38 (2007).
9. J. H. Davis, *Chem. Lett.*, **33**, 1072 (2004).
10. Y. Park, K. Y. A. Lin, A. H. A. Park and C. Petit, *Front. Energy Res.*, **3**, 42 (2015).
11. IEA Greenhouse Gas R&D Programme (IEA GHG). Evaluation of post-combustion CO_2 capture solvent concepts (2009).
12. A. Aroonwilas and P. Tontiwachwuthikul, *Sep. Purif. Technol.*, **12**, 67 (1997).
13. N. Dave, T. Do, G. Puxty, R. Rowland, P. H. M. Feron and M. I. Attalla, *Energy Procedia*, **1**, 949 (2009).
14. P. Scovazzo, D. Havard, M. McShea, S. Mixon and D. Morgan, *J. Membr. Sci.*, **327**, 41 (2009).
15. J. Ilconich, C. Myers, H. Pennline and D. Luebke, *J. Membr. Sci.*, **298**, 41 (2007).
16. S. Hanioka, T. Maruyama, T. Sotani, M. Teramoto, H. Matsuyama, K. Nakashima, M. Hanaki, F. Kubota and M. Goto, *J. Membr. Sci.*, **314**, 1 (2008).
17. C. Myers, H. Pennline, D. Luebke, J. Ilconich, J. K. Dixon, E. J. Maginn and J. F. Brennecke, *J. Membr. Sci.*, **322**, 28 (2008).
18. S. Yoo, J. Won, S. W. Kang, Y. S. Kang and S. Nagase, *J. Membr. Sci.*, **363**, 72 (2010).
19. L. A. Neves, J. G. Crespo and I. M. Coelhoso, *J. Membr. Sci.*, **357**, 160 (2010).
20. D. D. Iarikov, P. Hacarlioglu and S. T. Oyama, *Chem. Eng. J.*, **166**, 401 (2011).
21. D. Chinn, D. Q. Vu, M. S. Driver and L. C. Boudreau, US Patent US20,060,251,558A1, November 9 (2006).
22. D. Camper, J. E. Bara, D. L. Gin and R. D. Noble, *Ind. Eng. Chem. Res.*, **47**, 8496 (2008).
23. Y. Wang, C. Fang, F. Zhang, J. Geng, Y. Wu, J. Geng and Z. Zhang, *CIESC J.*, **60**, 2781 (2009).
24. A. Ahmady, M. A. Hashim and M. K. Aroua, *J. Chem. Eng. Data*, **55**, 5733 (2010).
25. Z. Feng, C. G. Fang, Y. T. Wu, Y. T. Wang, A. M. Li and Z. B. Zang, *Chem. Eng. J.*, **160**, 691 (2010).
26. C. Cadena, J. L. Anthony, J. K. Shah, T. I. Morrow, J. F. Brennecke and E. J. Maginn, *J. am. Chem. Soc.*, **126**, 5300 (2004).
27. S. H. Ha and Y. M. Koo, *Korean J. Chem. Eng.*, **28**, 2095 (2011).
28. D. W. Kim, R. Roshan, J. Tharun, A. Cherian and D. W Park, *Korean J. Chem. Eng.*, **30**, 1973 (2013).
29. J. E. Kim, H. J. Kim and J. S. Lim, *Fluid Phase Equilib.*, **367**, 151 (2014).
30. J. E. Kim, J. W. Kang and J. S. Lim, *Korean J. Chem. Eng.*, **32**, 1678 (2015).
31. H. N. Song, B. C. Lee and J. S. Lim, *J. Chem. Eng. Data*, **55**, 891 (2010).
32. S. A. Kim, J. H. Yim and J. S. Lim, *Fluid Phase Equilib.*, **332**, 28 (2012).
33. J. H. Yim and J. S. Lim, *Fluid Phase Equilib.*, **352**, 67 (2013).
34. J. M. Prausnitz, R. N. Lichtenthaler and E. G. de Azevedo, Molecular Thermodynamics of Fluid-Phase Equilibria, 3rd Ed., Prentice-Hall, NJ (1999).
35. M. O. McLinden, S. A. Klein, E. W. Lemmoon and A. P. Peskin, Thermodynamic Properties of Refrigerants and Refrigerant Mixtures Database (REFPROP) V.6.01, NIST, Gaithersburg, MD (1998).
36. J. O. Valderrama and R. E. Rojas, *Ind. Eng. Chem. Res.*, **48**, 6890 (2009).